

Xiaoming Zhao,
Yuanjun Liu*,
Tenglong Liang

Study on the Thermal Insulation Performance of PAN Pre-Oxidised Fibre Felts

DOI: 10.5604/01.3001.0013.9015

Tianjin Polytechnic University,
School of Textiles,
Tianjin 300387, P.R. China,
*e-mail: yankansd@163.com

Abstract

In this paper, an orthogonal experiment of 3 factors and 3 levels was firstly designed to prepare PAN pre-oxidised fibre felts with good thermal insulation properties; the range method was used to analyse the result of the orthogonal experiment, and finally the tensile properties and thermal stability were tested. Finally, pre-oxidised fibre felt composites for the coating of silica aerogel were prepared using the coating process to compound silica aerogel on re-oxidised fibre felts. Firstly, the influence of the content of silica aerogel on the heat insulation performance of the coated composite materials was analysed, and then a test of the coefficient of thermal conductivity, an experiment on the back temperature, and characterisations of the tensile properties and thermal stability of the composite coating of pre-oxidised fibre felt composites of the coating of silica aerogel were carried out. Results showed that through analysis of the orthogonal experiment, we can state that the best preparation process of pre-oxidised fibre needled felts was as follows: needle number – 2, needle depth – 8 mm, and needle frequency – 140 times/min. The transverse tensile strength of PAN pre-oxidised fibre needled felts prepared by crossly webbing of PAN pre-oxidised fibres was superior to the longitudinal tensile strength; thermogravimetric analysis showed that the pre-oxidised fibre needled felts had excellent thermal stability. The coefficient of thermal conductivity of the aerogel coating of the composites firstly decreased and then increased with an increase in the content of aerogel. Coated composites had the lowest coefficient of thermal conductivity when the aerogel content was 4% wt. At temperatures of 100 °C, 150 °C and 200 °C, the heating rate of the transient-state back temperature and the steady-state average temperature were both the lowest when the aerogel content was 6% wt.

Key words: pre-oxidised fibre felts, heat insulation performance, silica aerogel, coating, composite materials.

Introduction

PAN pre-oxidised fibre is a carbon fibre precursor obtained with polyacrylonitrile fibres through treatment from 180 °C to 300 °C in purifying air, which are referred to as pre-oxidised fibres or panof silks [1, 2]. In the process of the manufacture of carbon fibres, the pre-oxidised process plays the role of serving as a link between the past (PAN precursors) and the future (carbide carbonization). Due to the softening point temperature of PAN precursors being 104 °C, the decomposition temperature is 317 °C [3-5] in order not to make PAN precursors melt and burn in the process of carbonisation at high temperature. Firstly, pre-oxidised treatment is carried out, in the process of which the linear molecular chain structure of polyacrylonitrile experiences dehydrogenation and cyclisation, and transforms into a trapezoidal structure with good thermal stability [6-10].

The pre-oxidised process is carried out in a pre-oxidised furnace. The thermal stabilisation temperature, time, the heating speed of the heating system, the tension draft ratio of the drafting system, air supply, the hot air flow rate of the exhaust system, the flow velocity, flow

and temperature are important process parameters in the pre-oxidation process. The process parameters have a really major influence on the kinetics and thermodynamics of the pre-oxidised reaction, which directly affects the quality of PAN pre-oxidised fibre felts [11-13].

PAN pre-oxidized fibres are a type of heat-resisting fibres that emerged with the development of carbon fibres. They can be divided into two categories: one type is continuous filament bundles prepared specially as final products, while the other type is as intermediate products applied in heat preservation areas in the process of producing carbon fibres. However, some pre-oxidised fibres were abandoned due to technical parameters not meeting the requirements, and due to the low rate of domestic carbon fibres with high performance in the process of preparing carbon fibres [14-16]. Therefore, PAN pre-oxidised fibres as a final product and as an intermediate product not only have different controlled technology parameters but also various comprehensive technical indicators. Final products of pre-oxidised fibres have different performance requirements according to the different purposes, while intermediate products of pre-oxidised

fibres belong are non-combustible fibre due to their excellent thermal stability, high flame retardancy, the limited oxygen index being larger than 40%, and to not melting or bursting into flames. Moreover, they have a low coefficient of thermal conductivity, low cost, resistance to acid and alkali corrosion, resistance to a chemical environment, and good radiation resistance performance. They also have an important application value in the field of heat insulation, a textile processing performance unencumbered by inorganic heat resistant fibres, and they pose no harm to the human body, such as the harmful effects of asbestos [17, 18]. At present, PAN pre-oxidised fibres are mainly used in protective clothing, such as high temperature smocks, fire fighting, welding, fire gloves, fire ribbons, fire escape ropes, and flame retardant decorative materials like flame retardant heat curtains and seat covers for all types of vehicles.

Due to characteristics like poor electrical conductivity, low crimp, brittle fibre PAN pre-oxidised fibres, which leads to difficulty in turning fibres into articles, high breakage during the process of the spinning and weaving, low production efficiency and poor product quality, at

Table 1. Specification of pre-oxidised fibres.

| Average length, mm | Linear density, dtex | Average diameter, μm | Breaking strength, cN/dtex | Elongation at break, % | Crimp number crimp numbers/cm |
|--------------------|----------------------|---------------------------------|----------------------------|------------------------|-------------------------------|
| 51.00 | 1.66 | 12.40 | 1.53 | 18.29 | 4.40 |

present most pre-oxidised fibre products are mostly produced through nonwoven technology, especially needle nonwoven technology. The main technology for preparing pre-oxidised fibre felt is nonwoven needle processing technology. fibre where pre-oxidised fibres undergo the processes of opening, combing into a network, webbing and needling [19-21]. Many factors are needed to be considered to prepare pre-oxidised fibre felts with excellent heat insulation performance. Different production technologies produce variations in the properties of the heat insulation of pre-oxidised fibre felts. In order to probe into the influence of the production technology on the properties of the heat insulation of materials, a large number of experiments are needed to be carried out. For needed nonwoven pre-oxidised fibre felts, the web features, needle characteristics and needle technique all affect the structure of pre-oxidised fibre felts, thus being a major influence on the heat insulation of pre-oxidised fibre felts [22, 23].

Aerogel is a type of gel material that uses gases as the dispersive medium. There are many types, such as single phase aerogel, multiphase aerogel, organic aerogel and carbon aerogel. Silica aerogel is the most used material, due to its super light mass and translucent colour, which is referred to as "solid smoke", and it has hole of nanometers, with high porosity (larger than 99%), a high specific area (200-1000 m^2/g), low volume density (as low as 3 kg/m^3), an extremely low coefficient of thermal conductivity (as low as 0.013 $\text{W}/\text{m}\cdot\text{K}$), resistance to low temperature and high temperature (200-1400 $^\circ\text{C}$), an A class non-combustible property, and excellent environmental protection non-toxic properties, leading to it being regarded as the most promising material in the field of heat insulation [24-25].

Functional particles such as silica aerogel particles are added into the coating agent to prepare a thermal insulation coating, where the thermal insulation function is realised using the the impedance function of the thermal transfer. The prepared insulation composite material of fibre wiki with silica aerogel has advantages such

as a small specific gravity and low coefficient of thermal conductivity. For the thermal bonding composite process of adding silica aerogel (micro) particles in the process of the preparation of thermal bonding nonwoven cloth, the preparation method is simple and environmentally friendly, where functional particles combine with matrixes and dispersed evenly, which plays an effective role in the particle's thermal insulation effect [26-27]. The chemical bonding method can solve well the problem of moulding consolidation of silica aerogel (micro) particles with fibre materials, through choosing adhesives which are resistant to high temperature fibre, leading to thermal insulation composite materials of fibre wiki with silica aerogel being applied at high temperature. The impregnation process is simple and flexible, which is suitable for large-scale industrial production and formatting products of thermal insulation felts with aerogel. Moreover, they can solve the problem of the loss of functional particles by the technology of laminating woven fabrics of low thermal conductivity and resistance to high temperature on both sides [28-29].

The nonwoven fibre materials formed is a complex of air, fibres and water, whose thermal performance is the result of the collection and interaction of three components. Through composite coating technology, silica aerogel is introduced using air as the dispersion medium, which can regulate the comprehensive thermal performance of complexes under the condition of multicomponent components. The best balance point of the heat insulation performance of composites and usage of silica aerogel was found by preparing thermal insulation composite materials of fibre wiki of silica aerogel which can be used in a higher temperature environment, which was the research focus of this paper [30-32].

At first, in this paper, an orthogonal experiment of 3 factors and 3 levels was firstly designed to prepare PAN pre-oxidised fibre felts with good thermal insulation properties, and the range method was used to analyse the result of the orthogonal experiment. Finally, pre-oxidised fibre felt composites for the coating

of silica aerogel were prepared using the coating process to compound silica aerogel on re-oxidized fibre felts. The heat transfer behaviour and heat insulation performance of the composite material at different temperatures were mainly investigated.

Experimental

Main experimental material

PAN pre-oxidised fibres were provided by Tianjin Weiduwei Technology Co., LTD., the specific specifications of which are shown in *Table 1*.

Silica aerogel particles (particle size – 0.5 mm) were provided by Zhejiang Nano Science and Technology Co., LTD., cyclohexane (analytically pure AR) by Tianjin Fengchuan Chemical Technology Co., LTD., and organic silicone resin DC736 by Daokangning (Zhangjiagang) Silicone Co., LTD.

The average particle size of the silica aerogel purchased was 0.5 mm. Due to the too large particle size, it cannot be applied in the composite process of the coating as coating agent functional particles. In view of this, silica aerogel particles experienced the minimum of grinding when a high-energy nano impact mill was used, where the grinding time was 1 h. The eventual size of the silica aerogel particles was about 125 μm .

Main laboratory equipment

Am XFH opening machine (China Qingdao Jiaonan Knitting Machinery Factory), a WL-GS-A-500 type carding machine (China Taicang Shuangfeng Non-woven Equipment Co., LTD.), a WL-ZGSZ-Y-400 type needle machine (China Taicang Shuangfeng Non-woven Equipment Co., LTD.), a WL-ZGSZ-Z-400 type main needle-punching machine (China Taicang Shuangfeng Non-woven Equipment Co., LTD.), a HCTP11B type counter balance (Beijing Medical Scales Factory), a YG 141LA fabric thickness tester (Laizhou City Electronic Instrument Co., LTD.), a TPS 2500 s thermal constant analyser (Sweden Hot Disk Company), JF-976S type intelligent constant temperature heating units (Dongguan City Changanjinfeng Electronic Tool Factory), DM6801A type temperature recorder (Shenzhen Yishengshengli Technology Co., LTD.), a YG028 universal material testing machine (Wenzhou Fangyuan

Instrument Co., LTD.), and a TGA1000 thermogravimetric analyzer (Shanghai Precision Instrument Co., LTD.) were used.

Scheme of experiment

PAN pre-oxidised fibre needled felts are produced from PAN pre-oxidised fibres by the process of opening, combing into a network, cross webbing, pre-needling and main needling (multichannel).

Pre-oxidised fibres applied with an anti-static agent are needed to be combed into the network by a combing machine/fabrics produced by the carding machine are single-layer network, of a certain quantity and width which cannot meet the requirements. They need to be folded into thick wires through the web machine, and then subsequent processing is carried out. In this paper, the way of webbing used was cross webbing, and the number webbing layers was 30.

Fabrics after webbing are transferred to the pre-needle machine; the pre-needle process is mainly reinforcing the fabrics, which are highly fluffy and with a small force between fibre nets. After the pre-needle process, the fibre assemblies are transferred to the main needle-punching machine. The research emphasis in this paper was to explore the influence of the needle depth and frequency on the heat insulation performance of PAN pre-oxidised fibre felts.

Preparation of the coating of composite materials:

- Due to silica aerogel particles being extremely hydrophobic, the good solubility of the organic silicone resin in cyclohexane was considered. Consequently, cyclohexane was chosen as a solvent to compound the coating agent. The specific preparation process was as follows: the adhesive of organic silicone resin and solvent of cyclohexane were mixed at a mass ratio of 1:1.3, where the viscous organic silicone resin adhesive was completely dissolved in the solvent of cyclohexane, stirred with a glass rod, thus forming an emulsion. Silica aerogel particles were added, leading to silica aerogel particles accounting for a mass fraction of 2% to 10% of the emulsion. Silica aerogel particles dispersed in the emulsion were stirred with a glass rod, then the mixture was stirred mechanically for 30 minutes to disperse evenly. and finally the coating agent was prepared.

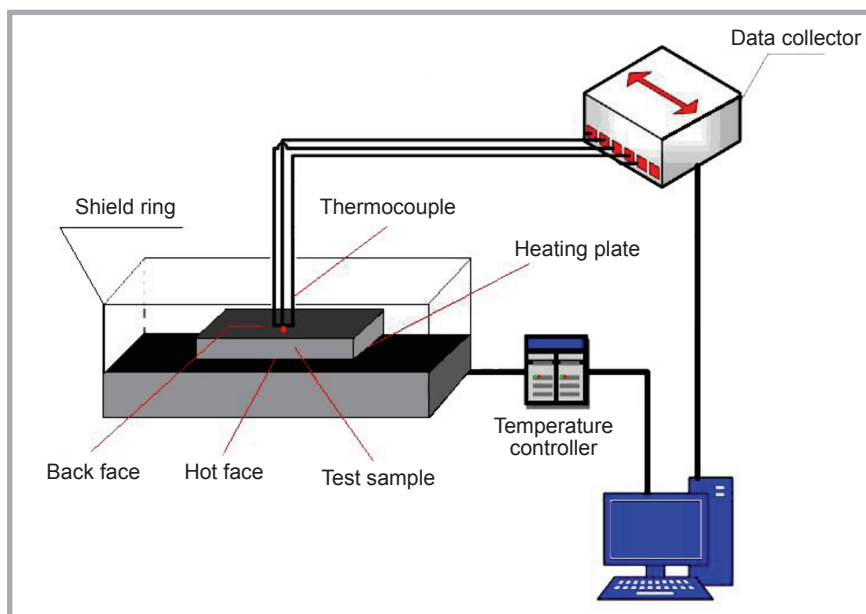


Figure 1. Schematic diagram of the test device of heat insulation.

- The coating agents prepared were used for coating pre-oxidised fibre felts, which were then tailored into ruled sizes on the coating machine; the coating was a single-sided layer of 0.4 mm thickness. Curing was performed for 24 hours at the indoor temperature, and finally composites of PAN pre-oxidised fibre felts with a coating of silica aerogel were prepared.

Testing and characterisation

Test of the coefficient of thermal conductivity

A test of the coefficient of thermal conductivity of the sample was carried out using a TPS 2500S thermal constant analyser in a lab at a constant temperature of 20 ± 1 °C and relative humidity of $65 \pm 5\%$. The test probe was a Hot Disk type 5465 polyimide coated film probe of 3.189 mm radius. The minimum sample size was an inscribed circle cylinder of 13 mm diameter and 3 mm height. The output power tested was 10 mw, and the heating time was 10 s.

Back temperature experiment

The test device for the back temperature is shown in Figure 1, where the size of the test sample is 50*50 mm, which makes the sample cover the heating plate. One piece of samples of each group of experiments is respectively tested on a heating plate at a temperature of 100 °C, 150 and 200 °C for 1800 s. At the corresponding constant temperature, 3 pieces of samples of each group of experiments are tested in total. Data of the back temperature of

the thermal insulation materials changing with time within the 1800 s are collected, with the thermocouple being placed in the centre position of the back of the samples. Through a lot of experimental analysis, the typically rising curve of the back temperature of the thermal insulation material gradually moves up with the increasing temperature of the heating plate. The typical process of the rise in temperature is divided into two parts: the transient and steady state. Before the test of 300 s, due to the sharp rise in the back temperature of the insulation materials, the rise rate of the temperature is faster, this process of the rapid change is defined as the transient state. Temperature data of the transient state is taken every 30 s. After 1500 s, a quasi-equilibrium state is arrived at in the thermal insulation materials due to the heat exchange with outside air, and the transient state is defined. The change in the back temperature of the thermal insulation materials changing with time is small when experiencing the transient state. Temperature data are collected every 300 s, and the average value of the five groups of temperature data for 600 s to 1800 s is defined as the average temperature of the transient state. In the transient phase, the size of the rise rate of the temperature is mainly used to evaluate the thermal insulation effect of materials, where the smaller the size of the rise rate of the temperature, the better the thermal insulation effect. The temperature difference between the heat surface temperature (the heating plate temperature) and the average temperature of the steady state of the thermal insulation ma-

Table 3. Results of the orthogonal experiment.

| Number | Needle frequency A, times/min | Needle number B, channel | Needle depth C, mm | Coefficient of thermal conductivity, W/(m·K) | Steady-state temperature difference when the temperature was 100 °C, °C | Steady-state temperature difference when the temperature was 150 °C, °C | Steady-state temperature difference when the temperature was 200 °C, °C |
|--------|-------------------------------|--------------------------|--------------------|--|---|---|---|
| 1 | 120 | 1 | 4 | 0.06121 | 29.2 | 48.0 | 60.8 |
| 2 | 120 | 2 | 6 | 0.06311 | 30.3 | 46.7 | 66.3 |
| 3 | 120 | 3 | 8 | 0.06311 | 30.7 | 49.7 | 65.8 |
| 4 | 170 | 1 | 6 | 0.06225 | 31.6 | 52.9 | 69.6 |
| 5 | 170 | 2 | 8 | 0.06124 | 26.5 | 48.2 | 65.8 |
| 6 | 170 | 3 | 4 | 0.06194 | 23.1 | 41.3 | 65.4 |
| 7 | 220 | 1 | 8 | 0.05982 | 26.1 | 45.0 | 65.5 |
| 8 | 220 | 2 | 4 | 0.06108 | 27.4 | 48.6 | 68.1 |
| 9 | 220 | 3 | 6 | 0.06263 | 20.1 | 37.9 | 45.1 |

Table 2. Design of the orthogonal experiment.

| Level | Needle frequency A, times/min | Needle number B, channel | Needle depth C, mm |
|-------|-------------------------------|--------------------------|--------------------|
| 1 | 80 | 1 | 4 |
| 2 | 110 | 2 | 6 |
| 3 | 140 | 3 | 8 |

Table 4. Analysis table of the orthogonal experiment using the coefficient of thermal conductivity as the performance index.

| Performance index | | A | B | C |
|--|--|----------------|----------------|---------|
| Coefficient of thermal conductivity | K _{1j} | 0.18743 | 0.18328 | 0.18423 |
| | K _{2j} | 0.18543 | 0.18543 | 0.18799 |
| | K _{3j} | 0.18353 | 0.18768 | 0.18417 |
| | k _{1j} | 0.06248 | 0.06109 | 0.06141 |
| | k _{2j} | 0.06181 | 0.06181 | 0.06266 |
| | k _{3j} | 0.06118 | 0.06256 | 0.06139 |
| | Range R _j | 0.0013 | 0.00147 | 0.00127 |
| | Primary and secondary order of factors B>A>C | | | |
| Optimal level | A ₃ | B ₁ | C ₃ | |
| Optimal combination A ₃ B ₁ C ₃ | | | | |

Table 5. Analysis table of the orthogonal experiment using the steady-state temperature difference as the performance index when the working temperature was 100 °C.

| Performance index | | A | B | C |
|---|--|----------------|----------------|-------|
| Steady-state temperature difference when the working temperature was 100 °C | K _{1j} | 90.2 | 86.9 | 79.7 |
| | K _{2j} | 81.2 | 84.2 | 82 |
| | K _{3j} | 73.6 | 73.9 | 83.3 |
| | k _{1j} | 30.07 | 28.97 | 26.57 |
| | k _{2j} | 27.07 | 28.07 | 27.33 |
| | k _{3j} | 24.53 | 24.63 | 27.77 |
| | Range R _j | 5.54 | 4.34 | 1.2 |
| | Primary and secondary order of factors A>B>C | | | |
| Optimal level | A ₁ | B ₁ | C ₃ | |
| Optimal combination A ₁ B ₁ C ₃ | | | | |

Table 6. Analysis table of the orthogonal experiment using the steady-state temperature difference as the performance index when the working temperature was 150 °C.

| Performance index | | A | B | C |
|---|--|----------------|----------------|-------|
| Steady-state temperature difference when the working temperature was 150 °C | K _{1j} | 144.4 | 195.9 | 137.9 |
| | K _{2j} | 142.4 | 143.5 | 137.5 |
| | K _{3j} | 131.5 | 128.9 | 142.9 |
| | k _{1j} | 48.13 | 48.63 | 45.97 |
| | k _{2j} | 47.47 | 47.83 | 45.83 |
| | k _{3j} | 43.83 | 42.97 | 47.63 |
| | Range R _j | 4.3 | 5.66 | 1.8 |
| | Primary and secondary order of factors B>A>C | | | |
| Optimal level | A ₁ | B ₁ | C ₃ | |
| Optimal combination A ₁ B ₁ C ₃ | | | | |

materials is defined as the temperature difference of the steady state in the steady phase, where the larger the temperature difference of the steady state, the better the thermal insulation effect.

Characterisation of tensile properties

In accordance with GB/T 24218.3-2010 (Textile Test Method for Nonwoven Cloth) part 3., characterisation of the tensile properties: breaking strength and elongation at break (strip method) of pre-oxidised fibre felts with better heat insulation performance was carried out. Five pieces of samples of the longitudinal (direction of the machine output) and transverse direction (vertical direction and output direction) were tested respectively, where the size of samples was 200 mm*50 mm +/- 0.5 mm. The tensile rate was set at 100 mm/min, and the specimen clamping distance was 100 mm, 5 pieces of samples of each group were tested and averaged.

Thermogravimetric analysis

A test of the thermal stability of pre-oxidized fibre felts with better heat insulation performance was carried out using a TGA1000 thermogravimetric analyser. The test atmosphere was N₂, and the heating rate – 10 °C/min.

Results and discussion

Determination of the optimal process parameter of pre-oxidised fibre felts with the good heat insulation performance

An orthogonal experiment of 3 factors and 3 levels was designed. A table of factor levels is shown in **Table 2**, and the results of the orthogonal experiment are shown in **Table 3**.

The orthogonal experimental results were analysed using the range method, the results of which are shown in **Tables 4, 5, 6** and **7**.

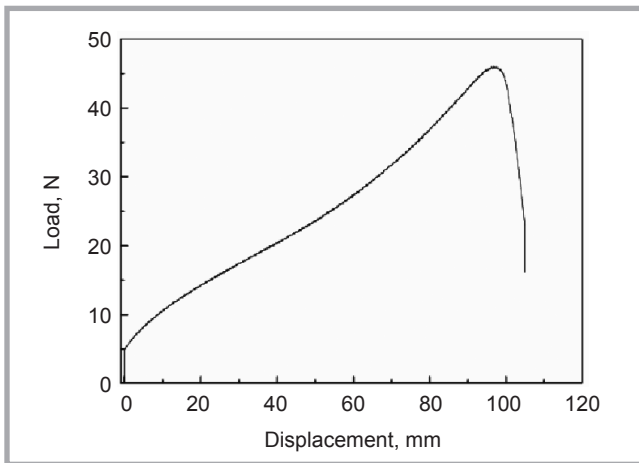


Figure 2. Longitudinal tensile displacement load diagram of pre-oxidised fibre needled felts.

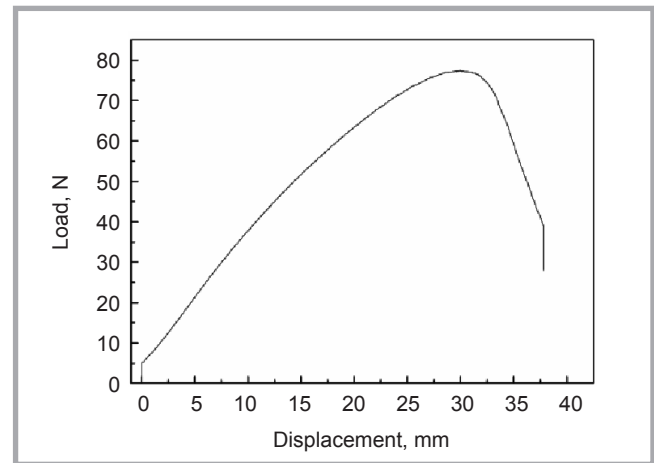


Figure 3. Transverse tensile displacement load diagram of pre-oxidised fibre needled felts.

We can see from **Table 4** that the primary and secondary order of factors influencing the coefficient of thermal conductivity of PAN pre-oxidised fibre felts at the indoor temperature was the needle number > the needle frequency > needle depth; the best optimal process condition leading to the lowest coefficient of thermal conductivity; namely, the best heat insulation performance at the indoor temperature was $A_3 B_1 C_3$.

We can see from **Table 5** that the primary and secondary order of factors influencing the steady-state temperature difference of PAN pre-oxidised fibre felts at a working temperature of 100 °C was needle frequency > the needle number > needle depth, and the best optimal process condition leading to the best heat insulation performance at a working temperature of 100 °C was $A_1 B_1 C_3$.

We can see from **Table 6** that the primary and secondary order of factors influencing the steady-state temperature difference of PAN pre-oxidised fibre felts at a working temperature of 150 °C was needle number > the needle frequency > needle depth, and the best optimal process condition leading to the best heat insulation performance of PAN pre-oxidised fibre felts at a working temperature of 150 °C was $A_1 B_1 C_3$.

Above all, the needle depth had a little influence on the heat insulation performance at an indoor temperature of 200 °C; however, proper needle depth can lead to vertical and horizontal hook enhancement, and at the same time, fibre fracture and breakage of prickers are not easily experienced. According

Table 7. Analysis table of the orthogonal experiment using the steady-state temperature difference as the performance index when the working temperature was 200 °C.

| Performance index | | A | B | C | |
|---|--|-------|-------|-------|--|
| Steady-state temperature difference when the working temperature was 200 °C | K_{1j} | 192.9 | 145.9 | 194.3 | |
| | K_{2j} | 200.8 | 200.2 | 181 | |
| | K_{3j} | 178.7 | 176.3 | 197.1 | |
| | k_{1j} | 64.3 | 48.63 | 64.77 | |
| | k_{2j} | 66.93 | 66.73 | 60.33 | |
| | k_{3j} | 59.57 | 58.77 | 65.7 | |
| | Range R_j | 7.36 | 18.1 | 5.37 | |
| | Primary and secondary order of factors $B > A > C$ | | | | |
| | Optimal level | A_2 | B_2 | C_3 | |
| Optimal combination $A_2 B_2 C_3$ | | | | | |

to the analysis of results of the orthogonal experiment, a needle depth of 8 mm was seen consistently as the best condition. Moreover, the influence of the needle number at an indoor temperature of 200 °C on the heat insulation performance was the most significant. In order to increase the strength of pre-oxidised fibre felts in line with the principle of improving the heat insulation performance, a needle number of 2 was chosen. A needle frequency of 140/min was

mainly considered for the smoothness of operation of the needle-punching machine, because though it guaranteed better heat insulation performance of the pre-oxidised fibre felts. The emergency stop of the needle-punching machine was also initiated. In conclusion, in this paper, in the research range of process parameters, a needle number of 2, a needle depth of 8 mm and a needle frequency of 140 times/min were chosen as the best process parameter.

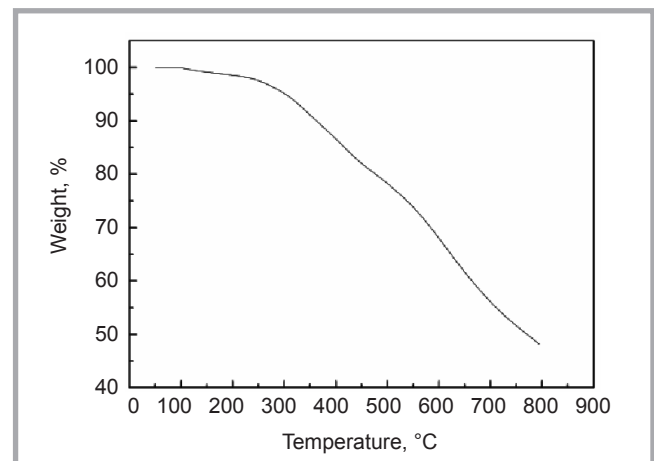


Figure 4. TG curve of pre-oxidised fibre felts.

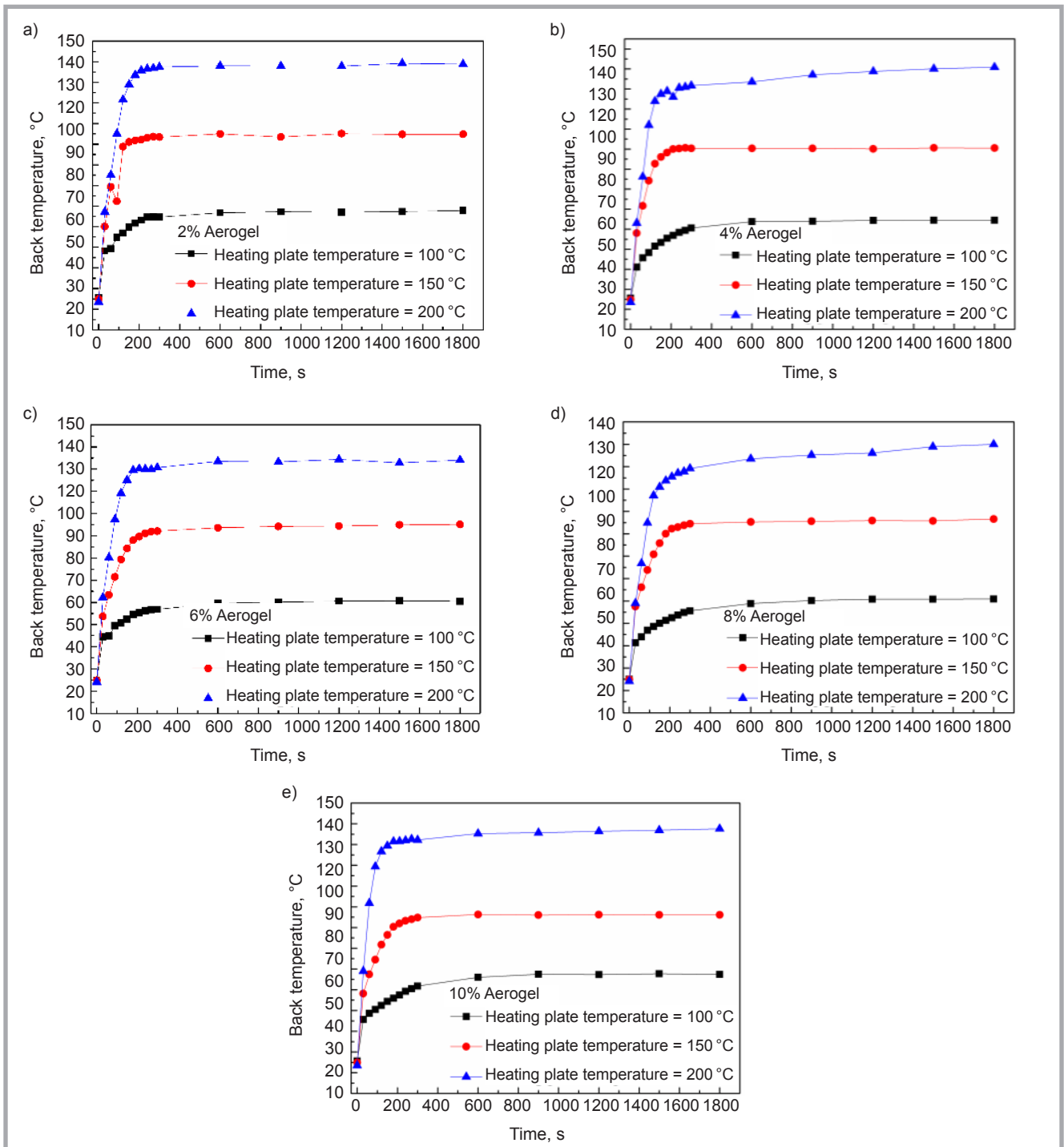


Figure 5. Heating process of the back temperature when the content of aerogel of the coated composites was 2-10%.

Performance characterisation of pre-oxidised fibre felts

Characterisation of tensile properties

Characterisation of the tensile properties of the pre-oxidised fibre felts prepared under conditions of the optimal process was carried out, which is shown in **Figure 2** and **Figure 3**, depicting longitudinal and transverse tensile displacement-load diagrams of pre-oxidized fibre felts, respectively. The figure shows that the longitudinal tensile breaking strength

was 46.1 N, the longitudinal elongation at break – 48.5%, the transverse rupture strength – 0.173 MPa; the transverse tensile breaking strength – 77.5 N, the transverse elongation at break – 15%, and the transverse rupture strength – 0.290 MPa. The transverse strength was larger than the longitudinal strength of pre-oxidized fibre felts, which was mainly because web technology was used as the method of cross webbing. If we observe the output direction of the web machine, most

of the fibres in the fabric are mainly arranged horizontally. The transverse distribution of pre-oxidised fibre felts in the transverse tensile process can share the greater tensile strength, leading to the tensile strength being greater than the longitudinal strength. Until the pre-oxidised fibre felts experience fracture, the transverse slippage between fibres was less than the longitudinal slippage, and led to the transverse elongation at break being less than the longitudinal elongation.

tion at break. But on the whole, the mechanical properties of pre-oxidised fibre needled felts was poor, with the mechanical properties mainly being weakened due to the technology of preoxidation, which led to the poor mechanical properties of the pre-oxidised fibre products.

Thermogravimetric analysis

In order to characterise the thermal stability of the pre-oxidised fibre felts prepared under conditions of the optimal technology, thermogravimetric analysis was carried out, being the relation of the mass of the materials measured changing with temperature (or time) under the control of the process temperature.

Figure 4 shows the TG curve of pre-oxidised fibre felts, where the abscissa is the heating temperature, and the ordinate was the percentage of the mass and the original mass. The weightlessness of pre-oxidized fibre felts was divided into two stages: the first phase was from 175.18 to 476 °C, where the weightlessness rate was 17.57%, and the second phase was from 476 to 732.39 °C, where the weightlessness rate was 25.26%. At a temperature of 412.66 and 619.07 °C, the maximums of the first and second weight loss rates were achieved, respectively. Overall, pre-oxidised fibre felts had excellent thermal stability when prepared with PAN pre-oxidised fibres.

Influence of the content of silica aerogels on the heat insulation performance of coated composites

Test results of the coefficient of thermal conductivity

DC736 adhesive of organic silicone resin and solvent of cyclohexane at a mass ratio of 1:1.3 were mixed into the emulsion, with silica aerogel accounting for 2%, 4%, 6%, 8% and 10% of the mass fraction of the emulsion.

Tests of the coefficient of thermal conductivity of the samples above were carried out, respectively, the results of which are shown in Table 8, depicting that the coefficient of thermal conductivity of coated composites with different contents of aerogel were all larger than that (0.06576 W/m·K) of the base cloth of the coated composites, which was mainly caused by the enhanced density of the composites after coating. With an increase in the percentage of aerogel, the coefficient of thermal conductivity showed a tendency of increasing first and then decreasing. The turning point

Figure 6. Influence of the aerogel content on the back temperature when the heating plate temperature was 100 °C.

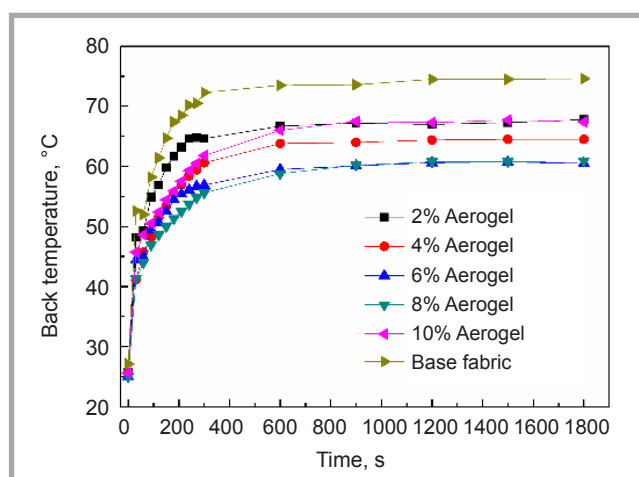


Table 8. Influence of the content of silica aerogel on the coefficient of thermal conductivity.

| Content of silica aerogel, % | Coefficient of thermal conductivity, W/(m·K) | Mean variation |
|------------------------------|--|----------------|
| 2 | 0.09027 | 0.00051 |
| 4 | 0.07504 | 0.00157 |
| 6 | 0.07692 | 0.00124 |
| 8 | 0.07857 | 0.00107 |
| 10 | 0.08405 | 0.00090 |

appeared when the percentage content of aerogel was 4% wt. When the content of aerogel was less than 4% wt, an increase in aerogel content had the effect of the insulation of heat transfer, which was mainly due to the hole size of aerogel of the nanometer level and the mean free path of gas molecules within the empty holes (the size of the insulation of the energy transmission) being the same. When even smaller, the holes will limit the movement of the gas molecules contained, which can greatly decrease heat convection, thereby reducing the overall thermal conductivity. Hence within a certain range, an increase in the content of aerogel reduced the coefficient of thermal conductivity of the coating of the composite material.

But when the aerogel content was greater than 4% wt, the heat insulation performance of the coated composite decreased, which was mainly due to that fact that the smaller the density of silica aerogel particles, the larger the content of aerogel particles, meaning that the aerogel volume added was larger, causing the coating agent to be more and more viscous, which led to poor dispersion of functional particles and the experiencing of the precipitation, and thus causing an increase in the coefficient of thermal conductivity and a decrease in the heat insulation performance. Hence, the test of the coefficient of thermal conductivity

at the indoor temperature showed that when the content of aerogel was 4% wt, PAN pre-oxidized fibre felt/silica aerogel composite material had the best heat insulation performance.

Experiment of the back temperature

In order to explore the heat transfer behaviour and heat insulation effect at different temperatures of different contents of aerogel (2%, 4%, 6%, 8% & 10%) of the PAN pre-oxidised fibre felt/silica aerogel composites, the heating plate temperature was set at 100 °C, 150 °C and 200 °C, respectively. Results of the experiment of the back temperature were recorded and are shown in Figures 5.a, 2.b, 2.c, 2.d and 2.e.

In order to further illustrate the influence of the aerogel content on the heat transfer behavior and heat insulation performance of the coated composites, the heating processes of the back temperature of coated composites of different contents of aerogel at the same temperature are given, respectively.

As shown in Figure 6, the heating plate temperature was set at 100 °C, then the heat transfer behaviour and heat insulation performance of coated composites of different contents of aerogel were examined, and a control experiment with the heat insulation performance of the base fabrics used in the coating was

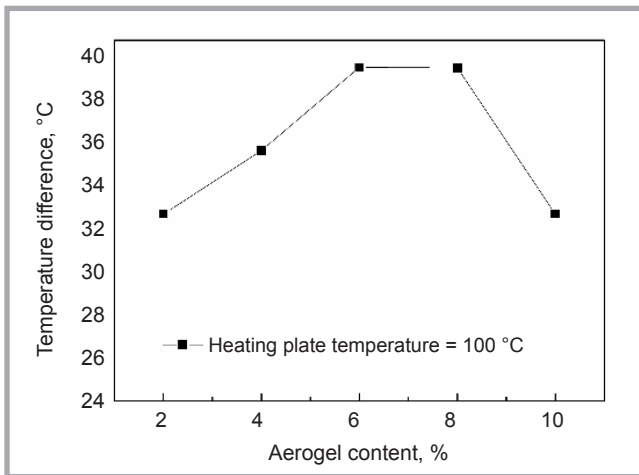


Figure 7. Influence of the aerogel content on the steady-state temperature difference.

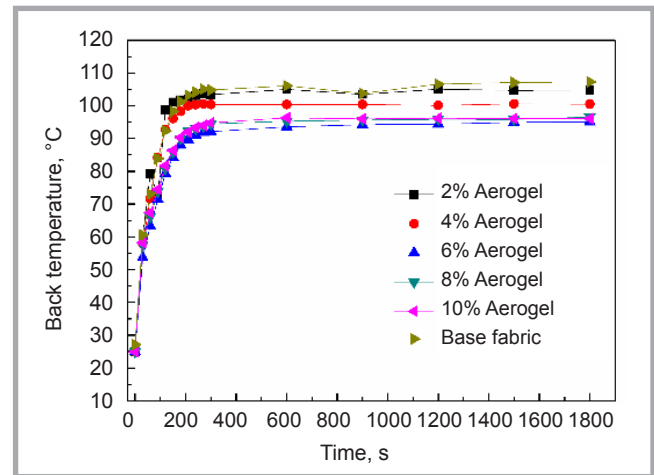


Figure 8. Influence of the aerogel content on the back temperature when the heating plate temperature was 150 °C.

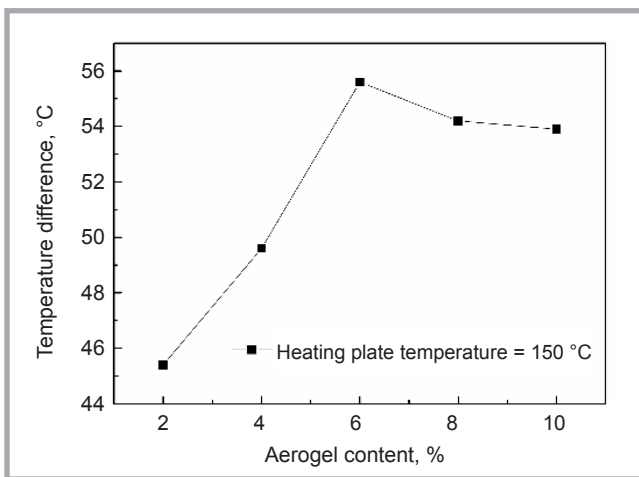


Figure 9. Influence of the aerogel content on the steady-state temperature difference.

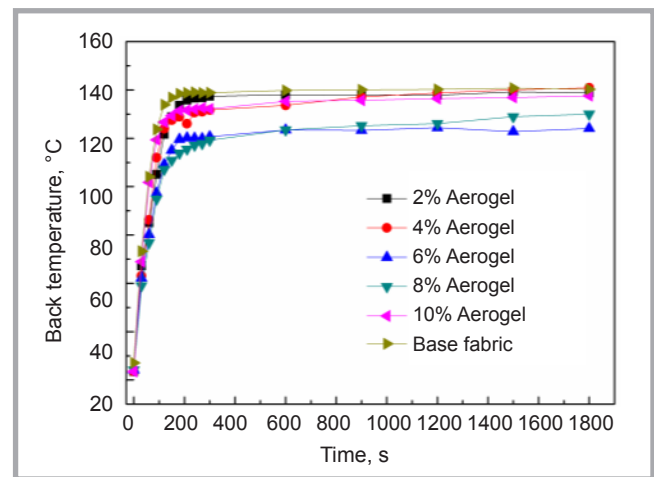


Figure 10. Influence of the aerogel content on the back temperature when the heating plate temperature was 200 °C.

carried out. Before the transient state of 30 s, the rising curves of the back temperature of each aerogel content of the coated composites overlapped, while in the transient state after this situation, the heating rates of the back temperature of the coated composites when the aerogel content was 6% wt and 8% wt, were lower and close to each other. From the point of the steady state, the steady-state temperature curves of the back temperature of the coated composites overlapped when the aerogel content was 6% wt and 8% wt and steady-state temperature was lower, where the steady-state average temperature was 60.28 °C and 60.3 °C, respectively. The heating rates of the back temperature and the values of the back steady-state temperature of coated composites of each aerogel content were significantly lower than those of the base fabric, with the lowest back steady-state average temperature being lower than that of the base fabric of 13.9 °C.

Figure 7 shows the influence of the aerogel content on the steady-state temperature difference when the heating plate temperature was 100 °C. Along with an increase in the aerogel content of the coated composites, the steady-state temperature difference increased first and then decreased. When the aerogel contents were 6% wt and 8% wt, the steady-state temperature differences were both larger, but not so large. The steady-state temperature difference was slightly larger when the aerogel content was 6% wt. The largest steady-state temperature difference was 39.7 °C, at which the steady-state heat insulation performance was the best. We can see from the heat transfer characteristic of the aerogel coated composites in a transient and steady state that when the working temperature was 100 °C and the aerogel content 6% wt, the coated composite had the optimal heat insulation performance.

As shown in **Figure 8**, the heating plate temperature was set at 150 °C. The heat transfer behaviour and heat insulation performance of coated composites of different contents of aerogel were examined, and a control experiment with the heat insulation performance of base fabrics with the coating was carried out. From the point of a transient state, the heating rate of the back temperature of the coated composites was the lowest when the aerogel content was 6% wt, while that of the back temperature of the base fabric without treatment of the coating was the largest. From the point of a steady state, the back temperatures of all aerogel coated composites were all lower than those of the base fabric, which confirmed the effectiveness of the insulation of heat flow of the aerogel coating. The back steady-state temperature was the lowest when the aerogel content was 6% wt. The minimum steady-state average temperature was

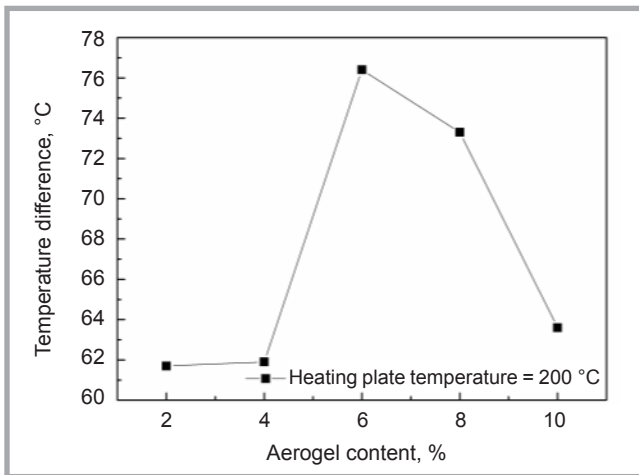


Figure 11. Influence of the aerogel content on the steady-state temperature difference.

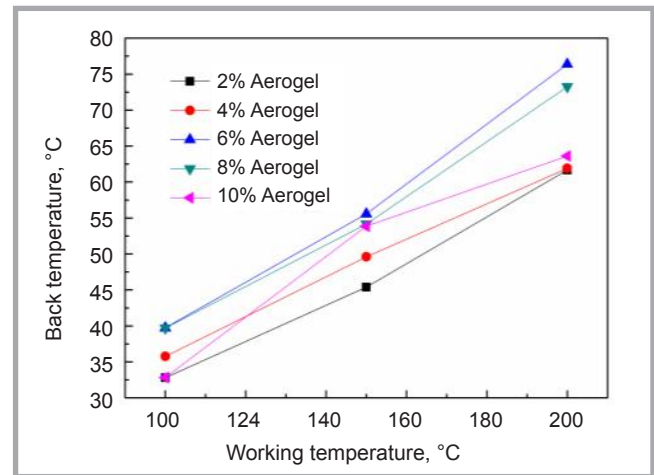


Figure 12. Influence of the working temperature on the steady-state temperature difference.

94.4 °C, which was lower than that of base cloth of 11.7 °C.

Figure 9 shows that when the heating plate temperature was 150 °C, there is an influence of the aerogel content on the steady-state temperature difference of the coated composites. Along with an increase in the aerogel content, the steady-state temperature difference of the coated composites first increased. When the aerogel content was 6% wt, the steady-state temperature difference was the largest, with a maximum value of 55.6 °C. When the aerogel content was increased again, the steady-state temperature difference of the coated composites showed a decreasing trend. The heat transfer behaviour of aerogel coated composites in a transient and steady state was considered comprehensively. When the working temperature was 150 °C and the aerogel content 6% wt, the coated composite had the optimal heat insulation performance.

As shown in **Figure 10**, the heating plate temperature was set at 200 °C. The heat transfer behaviour and heat insulation performance of PAN pre-oxidized fibre felt/silica aerogel composites at a working temperature of 200 °C was explored, and a control experiment with the heat insulation performance of base fabrics with the coating was carried out. From the point of a transient state, the heating rates of the back temperature of the coated composites were both lower when the aerogel contents were 6% wt and 8% wt. The heating rate of base fabric with the coating was the largest, which confirmed the effectiveness of the blockage of heat flow of the aerogel coating. From the point of a steady state, when the aerogel

content was 6% wt the back steady-state temperature of the coated composites was the lowest, where the lowest back steady-state average temperature was 123.6 °C. The steady-state temperatures of all aerogel coated composites were all lower than those of the base fabric, and the minimum steady-state average temperature was lower than that of base cloth of 16.6 °C.

Figure 11 shows that when the heating plate temperature was 200 °C, there was an influence of the aerogel content of the steady-state temperature difference of the coated composites. Along with an increase in the aerogel content, the steady-state temperature difference of the coated composites showed an increasing trend. When the aerogel content was 6% wt, the steady-state temperature difference was the largest, where the maximum value was 76.4 °C. After that, with an increase in the aerogel content, the steady-state temperature difference of the coated composites decreased gradually. The heat transfer characteristic of the aerogel coated composites in a transient and steady state was considered comprehensively when the working temperature was 200 °C. The coated composite had the optimal heat insulation performance when the aerogel content was 6% wt.

The heat transfer characteristics of coated composites of different contents of aerogel at different temperatures of 100 °C, 150 °C and 200 °C were analysed comprehensively, and it was found that with an increase in the aerogel content, the thermal insulation effect of the coated composites first increased and

then decreased, and when the aerogel content was 6% wt, the coated composite had the best heat insulation performance. The causes of this phenomenon was that to a certain extent within the scope of increasing the content of aerogel, holes of aerogel at the nanometer level brought a lot of still air, which greatly limited the heat convection, and silica aerogel itself was a poor conductor of the heat transfer, increasing its content in the composite within a certain scope, which can block part of the heat transfer. But with an increase in the aerogel content, the coating agent gradually became thick and unevenly distributed, leading to functional particles experiencing precipitation, which caused a decrease in the heat insulation performance of the materials.

Figure 12 shows the situation of the steady-state temperature difference of composites with a coating of silica aerogel at different temperatures. We can observe from the figure that with an increase in the working temperature, the steady-state temperature difference of composites with a coating of silica aerogel increased linearly. But in the discussion and analysis of this section, only the heat conduction and heat convection at higher temperature were considered, which can actually be seen from the analysis above. The thermal insulation effect of the coated composite of a single functional particle (silica aerogel) needs to be improved, which was mainly because at a higher working temperature, the infrared thermal radiation occupied a large part of the heat transfer, and silica aerogel almost had strong permeability at a near infrared of 3-8 μm at a relatively higher temperature.

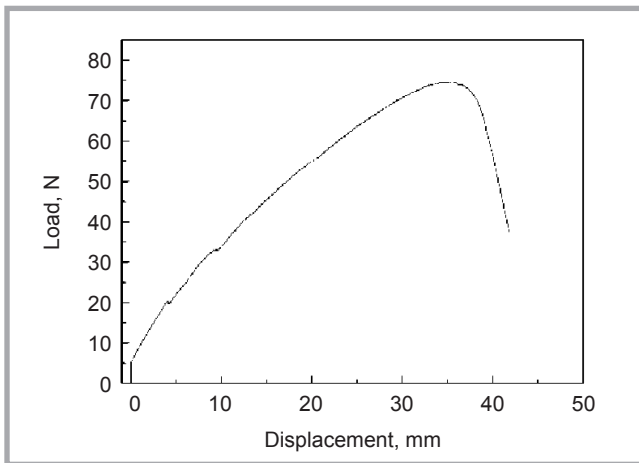


Figure 13. Displacement-load diagram of the aerogel coating of composites.

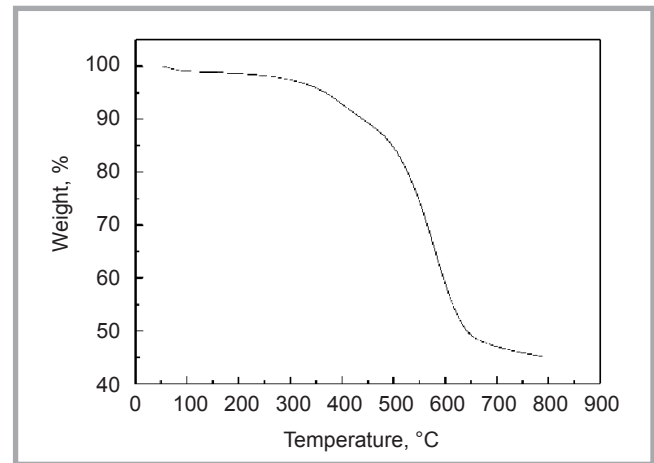


Figure 14. TG curve of the aerogel coating of the composites.

Performance characterisation of the aerogel composite coating

Characterisation of the tensile properties

A test of the longitudinal tensile properties of the coated composites was carried out when the aerogel content was 6% wt, the displacement-load diagram of which is shown in **Figure 13**. The figure shows that the tensile breaking strength was 74.7 N, the strength 0.26 MPa, and the elongation at break 17.8%. After pre-oxidized fibre felts were compounded with the aerogel, the composite showed better mechanical properties than pure pre-oxidized fibre felts (in the longitudinal direction), which was mainly due to the adhesive contained in the coating agent, leading to fragile pre-oxidized fibre felts obtaining a certain degree of enhancement. But aerogel is used as a type of flexible coating, and herein when the coating thickness was thinner, the improvement in the mechanical properties of the composite brought by the coating was not too large.

Thermogravimetric analysis

Figure 14 shows a TG curve of the coated composite when the aerogel content was 6% wt. We can see from **Figure 11** that the initial decomposition temperature of the aerogel coated composites was 336.62 °C, and the weightlessness rate from a temperature of 429.87 °C to 623.68 °C was 37.65%. The first and second maximum weight loss rates were respectively reached at temperatures of 391.09 °C and 573.87 °C. Overall, the aerogel coated composites had good thermal stability.

Conclusions

- (1) Based on the single factor experiment, an orthogonal experiment of 3 factors and 3 levels was designed. The best preparation technology was a needle number of 2, a needle depth of 8 mm and needle frequency of 140 times/min, established through the orthogonal experiment analysis of pre-oxidized fibre needled felts.
- (2) The test of the tensile properties showed that the transverse tensile strength was superior to the longitudinal tensile strength of pre-oxidized fibre needled felts prepared with PAN pre-oxidized fibres through cross webbing. On the whole, the tensile strength of PAN pre-oxidized fibre needled felts was lower; the thermogravimetric analysis showed that pre-oxidized fibre needled felts had excellent thermal stability.
- (3) The test of the coefficient of thermal conductivity showed that values of the coefficient of thermal conductivity of aerogel coated composites were all larger than that of the base fabric, where the coefficient of thermal conductivity of the aerogel coated composites first increased and then decreased with an increase in aerogel content. The coated composite had the lowest coefficient of thermal conductivity when the aerogel content was 4% wt.
- (4) When the working temperatures were 100 °C, 150 °C and 200 °C, the heating rate of the transient-state back temperature and the steady-state average temperature were both the smallest. When the aerogel content was 6% wt, the steady-state temper-

ature difference first increased and then decreased with the increasing of aerogel content, and the steady-state temperature difference was the largest when the aerogel content was 6% wt, and the heat insulation performance was the best. The steady-state temperature difference of the aerogel coated composite increased linearly with the increasing of working temperatures, and the heat insulation performance of transient and steady states of coated composites of each aerogel content at the corresponding temperatures was superior to that of the base fabric.

- (5) The test of the tensile properties showed that the tensile performance of pre-oxidized fibre felts after the coating process of compounding aerogel was further improved, which mainly benefited from the good adhesive performance of the organic silicone resin. the thermogravimetric analysis showed that the aerogel coated composite had good thermal stability.

Acknowledgements

The authors would like to acknowledge Project No. 2019TQ0181, 18JCTPJC62500, 18JCZDJC99900, 18JCYBJC86600, TJPJ2 K20170105, and 2017KJ070.

References

1. Stamopoulos AG, Tserpes KI, Prucha P, et al. Evaluation of Porosity Effects on the Mechanical Properties of Carbon Fiber-Reinforced Plastic Unidirectional Laminates by X-Ray Computed Tomography and Mechanical Testing[J]. *J. Compos. Mater.* 2016; 50: 2087-2098.

2. Takahashi F, Abbott A, Murray T M, *et al.* Thermal Response Characteristics of Fire Blanket Materials[J]. *Fire Mater.* 2014; 38: 609-638.
3. Liu SP, Han KQ, Chen L, *et al.* Influence of External Tension on the Structure and Properties of Melt-Spun PAN Precursor Fibers During Thermal Oxidation[J]. *J. Ind. Text.* 2015; 300: 1001-1009.
4. Zargham S, Bazgir S, Katbab AA, *et al.* High-Quality Carbon Nanofiber-Based Chemically Preoxidized Electrospun Nanofiber[J]. *Fuller. Nanotub. Car. N.* 2015; 23: 1008-1017.
5. Trautwein G, Plaza-Recobert M, Alcaniz-Monge J. Unusual Pre-Oxidized Polyacrylonitrile Fibres Behaviour Against their Activation with CO₂: Carbonization Effect[J]. *J. Alcaniz-Monge, Adsorption.* 2016; 22: 223-231.
6. Zhai YJ, Peng ZJ, Ren XB, *et al.* Effect of In-Situ Transformed Pre-Oxidized Polyacrylonitrile Fibers on the Microstructure and Mechanical Properties of Ticn-Based Cermets[J]. *Rare Metal. Mat. Eng.* 2015; 44: 731-734.
7. Ghelich R, Aghdam RM, Torknik FS, *et al.* Carbothermal Reduction Synthesis of Zrb₂ Nanofibers Via Pre-Oxidized Electrospun Zirconium N-Propoxide[J]. *Ceram. Int.* 2015; 41: 6905-6911.
8. Gao L L, Lu H Y, Lin H B, *et al.* KOH Direct Activation for Preparing Activated Carbon Fiber from Polyacrylonitrile-Based Pre-Oxidized Fiber[J]. *Chem. Res. Chinese U.* 2014; 30: 441-446.
9. Ren X M, Wang Y S, He T, *et al.* Analysis and Characterization of Orientation Structure of Pre-Oxidized PAN Fibers in High Magnetic Fields[J]. *J. Wuhan Univ. Technol.* 2014; 29: 224-228.
10. Chen LC, Peng P, Lin LF, *et al.* Facile Preparation of Nitrogen-Doped Activated Carbon for Carbon Dioxide Adsorption[J]. *Aerosol Air Qual. Res.* 2014; 140: 63-72.
11. Alam M, Singh H, Suresh S, *et al.* Energy and Economic Analysis of Vacuum Insulation Panels (Vips) used in Non-Domestic Buildings[J]. *Appl. Energy.* 2017; 188: 1-8.
12. Tomboulia BN, Hyers RW. Predicting the Effective Emissivity of an Array of Aligned Carbon Fibers using the Reverse Monte Carlo Ray-Tracing Method[J]. *J. Heat Trans-t. Asme.* 2017; 139: 012701.
13. Ao W, Liu P J, Yang W J. Agglomerates, Smoke Oxide Particles, and Carbon Inclusions in Condensed Combustion Products of an Aluminized GAP-Based Propellant[J]. *Acta Astronaut.* 2016; 129: 147-153.
14. Puzkarz AK, Krucińska I. Study of Multilayer Clothing Thermal Insulation Using Thermography and the Finite Volume Method. *FIBRES & TEXTILES in Eastern Europe* 2016; 24, 6(120): 129-137. DOI: 10.5604/12303666.1221747.
15. Gao C, Huang L, Yan L B, *et al.* Behavior of Glass and Carbon FRP Tube Encased Recycled Aggregate Concrete with Recycled Clay Brick Aggregate[J]. *Compos. Struct.*, 2016; 155: 245-254.
16. Lin JH, Chuang YC, Huang CH, *et al.* Needle-Bonded Electromagnetic Shielding Thermally Insulating Nonwoven Composite Boards: Property Evaluation-s[J]. *Appl. Sci-basel* 2016; 6: 303.
17. Vo L T T, Navard P. Treatments of Plant Biomass for Cementitious Building Materials – A Review[J]. *Constr. Build. Mater.* 2016; 121: 161-176.
18. Cheng HM, Hong CQ, Zhang XH, *et al.* Super Flame-Retardant Lightweight Rime-Like Carbon-Phenolic Nanofoam[J]. *Sci. Rep-UK* 2016; 6: 33480.
19. Li C D, Li B B, Pan N, *et al.* Thermo-Physical Properties of Polyester Fiber Reinforced Fumed Silica/Hollow Glass Microsphere Composite Core and Resulted Vacuum Insulation Panel[J]. *Energ. Buildings* 2016; 125: 298-309.
20. Williams J, Lawrence M, Walker P. A Method for the Assessment of the Internal Structure of Bio-Aggregate Concretes[J]. *Constr. Build. Mater.* 2016; 116: 45-51.
21. Silva HP, Pardini LC, Bittencourt E. Shear Properties of Carbon Fiber/Phenolic Resin Composites Heat Treated at High Temperatures[J]. *Aerosp. Sci. Technol.* 2016; 8: 363-372.
22. Pehlivanli Z O, Uzun I, Yuçel Z P, *et al.* The Effect of Different Fiber Reinforcement on the Thermal and Mechanical Properties of Autoclaved Aerated Concrete[J]. *Constr. Build. Mater.* 2016; 112: 325-330.
23. Martinelli E, Perri F, Sguazzo C, *et al.* Cyclic Shear-Compression Tests on Masonry Walls Strengthened with Alternative Configurations of CFRP Strips[J]. *B. Earthq. Eng.* 2016; 14: 1695-1720.
24. Shakir AS, Guan ZW, Jones SW. Lateral Impact Response of the Concrete Filled Steel Tube Columns with and without CFRP Strengthening[J]. *Eng. Struct.* 2016; 116: 148-162.
25. Ghelich R, Aghdam RM, Torknik FS, Jahanama MR, Keyanpour-Rad M. Carbothermal Reduction Synthesis of Zrb₂ Nanofibers Via Pre-Oxidized Electrospun Zirconium N-Propoxide. *Ceram Int* 2015; 41(5): 6905-6911.
26. Ren XM, Wang YS, He T, Xia ZC. Analysis and Characterization of Orientation Structure of Pre-Oxidized PAN Fibers in High Magnetic Fields. *J Wuhan Univ Technol* 2014; 29: 224-228.
27. Ao W, Liu P J, Yang WJ. Agglomerates, Smoke Oxide Particles, and Carbon Inclusions in Condensed Combustion Products of an Aluminized GAP-Based Propellant. *Acta Astronaut* 2016; 129: 147-153.
28. Gao C, Huang L, Yan L B, Kasal B, Li W G. Behavior of Glass and Carbon FRP Tube Encased Recycled Aggregate Concrete with Recycled Clay Brick Aggregate. *Compos Struct* 2016; 155: 245-254.
29. Chen LC, Peng PY, Lin LF, Yang TCK, Huang CM. Facile Preparation of Nitrogen-Doped Activated Carbon for Carbon Dioxide Adsorption. *Aerosol Air Qual Res* 2014; 140: 63-72.
30. Tomboulia BN, Hyers RW. Predicting the Effective Emissivity of an Array of Aligned Carbon Fibers Using the Reverse Monte Carlo Ray-Tracing Method. *J Heat Trans-t Asme* 2017; 139: 012701.
31. Lin JH, Chuang YC, Huang CH, Li TT, Huang CL, Chen YS, Lou CW. Needle-Bonded Electromagnetic Shielding Thermally Insulating Nonwoven Composite Boards: Property Evaluations. *Appl Sci-Basel* 2016; 6: 303.
32. Cheng HM, Hong CQ, Zhang XH, Xue HF, Meng SH, Han JC. Super Flame-Retardant Lightweight Rime-Like Carbon-Phenolic Nanofoam. *Sci Rep-UK* 2016; 6: 33480.
33. Williams J, Lawrence M, Walker P. A Method for the Assessment of the Internal Structure of Bio-Aggregate Concretes. *Constr Build Mater* 2016; 116: 45-51.

Received 18.09.2017 Reviewed 26.06.2019





XIII International Invention and Innovation Show INTARG® 2020



Spodek / International Conference Centre in Katowice, Poland